

Photophysics of Ion Clusters Formed between $[\text{Ru}(\text{bpy})_3]^{2+}$ and the Polyoxotungstate Anion $[\text{S}_2\text{W}_{18}\text{O}_{62}]^{4-}$

Michael K. Seery,[†] Liz Guerin,[†] Robert J. Forster,[†] Etienne Gicquel,^{†,||} Victoria Hultgren,[‡] Alan M. Bond,[‡] Anthony G. Wedd,[§] and Tia E. Keyes*,[†]

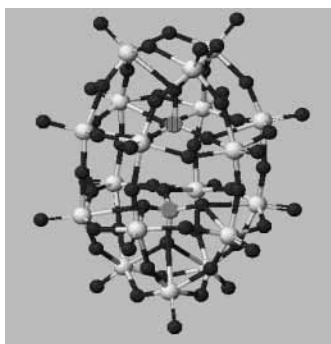
National Center for Sensors Research, School of Chemical Sciences, Dublin City University, Glasnevin, Dublin 9, Ireland, School of Chemistry, Monash University, Clayton, Victoria 3800, Australia, and School of Chemistry, University of Melbourne, Victoria 3010, Australia

Received: April 22, 2004; In Final Form: July 2, 2004

The interactions between $[\text{Ru}(\text{bpy})_3]^{2+}$ and the polyoxotungstate anion $[\text{S}_2\text{W}_{18}\text{O}_{62}]^{4-}$ in acetonitrile solution were investigated using a combination of photophysics and optical and Raman spectroscopies. The presence of ion clusters of $\{[\text{Ru}(\text{bpy})_3][\text{S}_2\text{W}_{18}\text{O}_{62}]\}^{2-}$ ($K_2 = 7.7 \times 10^5$) and $[\text{Ru}(\text{bpy})_3]_2[\text{S}_2\text{W}_{18}\text{O}_{62}]$ ($K_1 = 1.0 \times 10^6 \text{ mol}^{-2} \text{ dm}^{-6}$) are inferred. The 2:1 complex is weakly luminescent, with a lifetime at room temperature of 20 ns under aerobic conditions. Difference electronic absorption, excitation, and resonance Raman spectroscopies indicate that the tungstate anion participates in this transition. Under conditions where $[\text{Ru}(\text{bpy})_3]^{2+}$ alone is photolabile, the ion clusters are photostable, with no photodecomposition or photoinduced ligand exchange reactions evident in acetonitrile. This characteristic is examined employing temperature-dependent luminescent studies which demonstrate that the observed activation energy and preexponential factor are considerably different from those of free $[\text{Ru}(\text{bpy})_3]^{2+}$ and are characteristic of a photostable polypyridylruthenium complex.

Introduction

Heteropolyoxyometalates have received much attention due to their rich redox chemistry, their photochemistry, and their increasing application across areas as diverse as catalytic chemistry and medicinal chemistry.¹ The polyoxometalate anions $[\alpha\text{-S}_2\text{M}_{18}\text{O}_{62}]^{4-}$ ($\text{M} = \text{Mo}, \text{W}$; Dawson structure shown) contain sulfur as the central heteroatom and may be activated



photochemically through ligand to metal charge transfer to generate powerful oxidants.

The ability of the photoexcited anions to accept electrons from organic substrates such as benzyl alcohol, ethanol, and menthol has been demonstrated in photoelectrochemical studies.² However, these materials are predominantly ultraviolet absorbers and are not strongly activated by visible light, which presents a significant drawback in practical applications.^{2,3} As a consequence, we have been investigating the possibility of combining

these anions with visible photosensitizers based on simple polypyridylruthenium(II) complexes. $[\text{Ru}(\text{bpy})_3]^{2+}$ in particular is deemed to be a suitable candidate due to its strong absorption in the visible region and its well-characterized photophysical properties. Recently, we demonstrated that $[\text{Ru}(\text{bpy})_3]^{2+}$ and $[\text{S}_2\text{Mo}_{18}\text{O}_{62}]^{4-}$ combine to form both 1:1 and 2:1 ion clusters in acetonitrile solution. Significant electronic communication between the ions was detected in $[\text{Ru}(\text{bpy})_3]_2[\text{S}_2\text{Mo}_{18}\text{O}_{62}]$, including observation of a new optical transition at 485 nm, assigned to charge transfer from $[\text{Ru}(\text{bpy})_3]^{2+}$ to $[\text{S}_2\text{Mo}_{18}\text{O}_{62}]^{4-}$.

In the present paper, we report the electronic and photophysical properties of the equivalent adducts formed in acetonitrile with the tungstate analogue $[\text{S}_2\text{W}_{18}\text{O}_{62}]^{4-}$. Again, strong electronic communication between the ions appears to be a feature of these ion clusters, but in contrast to the polymolybdate system, a relatively long-lived luminescent charge-transfer component is detected. Compared to the photolability of $[\text{Ru}(\text{bpy})_3]^{2+}$, these ion clusters are robustly photostable. Two possible explanations are apparent. Either cluster formation grossly perturbs the molecular orbitals involved in the excited state, or the existing ^3MC (triplet metal centered) state has become thermally inaccessible. These possibilities are explored by temperature-dependent photophysical studies on the $[\text{Ru}(\text{bpy})_3]_2[\text{S}_2\text{W}_{18}\text{O}_{62}]$ cluster to provide further insight into the stabilizing effect of the polyoxometalate anion on $[\text{Ru}(\text{bpy})_3]^{2+}$.

Experimental Section

Materials. $[(\text{C}_6\text{H}_{13}\text{N})_4[\text{S}_2\text{Mo}_{18}\text{O}_{62}]]$, $[(\text{C}_6\text{H}_{13}\text{N})_4[\text{S}_2\text{W}_{18}\text{O}_{62}]]$, and $[\text{Ru}(\text{bpy})_3]\text{Cl}_2$ were synthesized according to published methods.^{5–7} $[\text{Ru}(\text{bpy})_3]_2[\text{S}_2\text{W}_{18}\text{O}_{62}]$ was prepared using a procedure analogous to that reported for $[\text{Ru}(\text{bpy})_3]_2[\text{S}_2\text{W}_{18}\text{O}_{62}]$.⁸ HPLC grade acetonitrile, 99.9%, obtained from Sigma-Aldrich was dried over molecular sieves, 3A, and was employed for all photochemical studies. Temperature-dependent studies were

[†] Dublin City University.

[‡] Monash University.

[§] University of Melbourne.

^{||} Current address: Université Libre de Bruxelles, Physical Organic Chemistry, CP 160/08, Av F. D. Roosevelt, 50 B-1050 Bruxelles, Belgium.

conducted in spectroscopic grade propionitrile/butyronitrile (4:5 v/v) purchased from Sigma-Aldrich. All other reagents, purchased from Sigma-Aldrich, were used as received.

Methods. Steady state emission spectra were recorded employing a Perkin-Elmer LS50B luminescence spectrometer. Time-resolved luminescence studies were conducted with an Edinburgh Instruments F900 time correlated single photon counting system or a custom-built laser photolysis system. In the latter system, luminescent lifetimes were measured using the second (532 nm, 50 mJ/pulse) or third harmonic (355 nm, 30 mJ/pulse) of a Continuum Surelite Q-switched Nd:YAG laser for excitation. Emission was detected in a right-angled configuration to the laser using an Andor Model M20 gated intensified CCD coupled to an Oriel Model MS125 spectrograph. With suitable signal averaging, this configuration allows a complete emission spectrum (spectral range 250 nm) to be obtained within times as short as 10 ns. The emission spectra were typically recorded using the average of 10 laser shots. The gate width, i.e., the exposure time of the CCD, was never more than 5% of the excited state lifetime. The step size, i.e., the time between the acquisition of discrete spectra, was typically 5% of the excited state half-life. Time-resolved absorption spectra were collected using the same instrumentation in absorption mode with an Oriel 300 W Xe arc lamp acting as the monitoring source. In this instance, spectra were typically recorded using the average of 25 laser shots. The gate width, i.e., the exposure time of the CCD, was never more than 10% of the excited state lifetime.

Temperature-dependent luminescent lifetimes were conducted in butyronitrile/propionitrile 4:5 v/v solution employing an Oxford Instruments Optistat DN cryostat. Samples were degassed with argon for at least 30 min prior to photomeasurement.

Absorption spectra were measured using a Shimadzu 3100 UV-vis/NIR spectrophotometer.

Raman spectroscopy was conducted on a Dilor Jobinyvon Spex Labram. The exciting Ar ion laser (514, 488, or 457.9 nm) was focused into the cell or onto a solid sample using a 10 \times objective lens. A spectral resolution of 1.5 cm⁻¹ per pixel was achieved using a grating of 1800 lines/mm, and the *x*-axis was calibrated against acetonitrile.

Computations, such as spectral fitting and extraction of lifetime data, were conducted using standard iterative techniques on Microsoft Excel.⁹

Results and Discussion

Luminescence Spectroscopy. To explore the impact of [S₂W₁₈O₆₂]⁴⁻ on the photophysics of [Ru(bpy)₃]²⁺, steady state quenching studies were conducted (Figure 1) in dry acetonitrile. As observed for the interaction of [S₂Mo₁₈O₆₂]⁴⁻ with [Ru(bpy)₃]²⁺, addition of increasing concentrations of [S₂W₁₈O₆₂]⁴⁻ resulted in significant quenching of the [Ru(bpy)₃]²⁺ excited state. The luminescence intensity of [Ru(bpy)₃]²⁺ (5 \times 10⁻⁶ M) decreased progressively with increasing concentrations of [S₂W₁₈O₆₂]⁴⁻. An isoemissive point at 545 nm was observed for tungstate concentrations in the range (0–4) \times 10⁻⁶ M, but was lost at higher concentrations. Concomitantly, the emission underwent a bathochromic shift, from 611 to 630 nm. This shift is less than that observed for the equivalent polymolybdate system, but is considerably more than that reported (4 nm) by Ballardini et al.¹⁰ for interactions between [Ru(bpy)₃]²⁺ and the Keggin anion [(HO–Mn)·PW₁₁O₃₉]⁶⁻.

The nature of the interaction in the tungstate system was probed by addition of LiClO₄ to solutions of the adduct. Perchlorate is known to associate very strongly with [Ru-

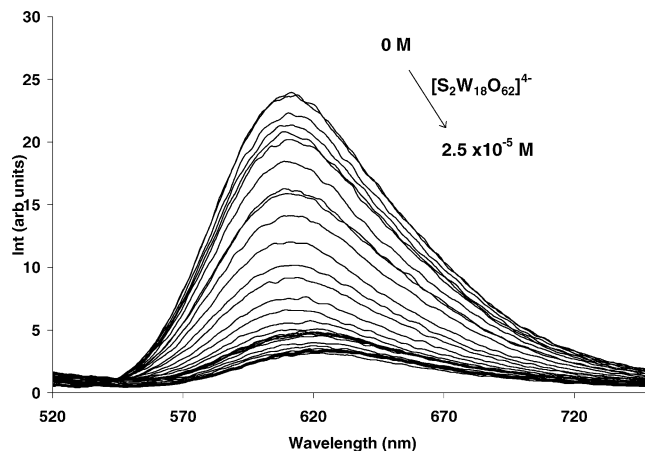


Figure 1. Luminescence spectrum (uncorrected) in dry acetonitrile of [Ru(bpy)₃]²⁺ (5 \times 10⁻⁶ M) on addition of [S₂W₁₈O₆₂]⁴⁻; excitation wavelength 450 nm.

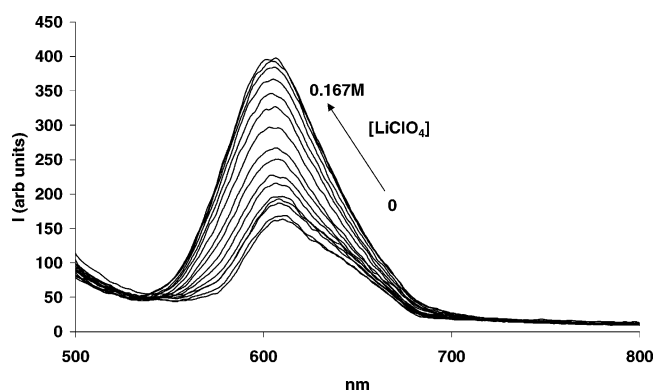
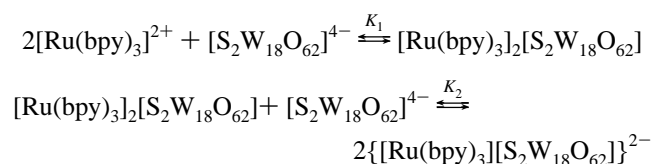


Figure 2. Influence of increasing solution ionic strength on quenching of [Ru(bpy)₃]²⁺ by [S₂W₁₈O₆₂]⁴⁻ in acetonitrile.

(bpy)₃]²⁺, and it is likely that the Li⁺ ion will ion pair with the polyoxometalate. Hence, at appropriate concentrations, LiClO₄ would be expected to disrupt the ion clusters if binding is purely electrostatic in nature. A solution containing a 2:1 ratio of [Ru(bpy)₃]²⁺ (2 \times 10⁻⁵ M) and [S₂W₁₈O₆₂]⁴⁻ (1 \times 10⁻⁵ M) was titrated with a solution of 1 M LiClO₄ (to minimize volume changes); see Figure 2. With increasing addition of salt, the luminescence intensity of the solution increased until it maximized at 0.167 mol dm⁻³ LiClO₄. At this concentration, the luminescence intensity was indistinguishable from that of free [Ru(bpy)₃]²⁺. Addition of LiClO₄ does not alter the luminescence intensity of [Ru(bpy)₃]²⁺.⁵ This behavior is comparable with that noted for the [Ru(bpy)₃]²⁺/[S₂Mo₁₈O₆₂]⁴⁻ system; however, in this instance only 0.05 mol dm⁻³ LiClO₄ was needed to regain the luminescent intensity.⁵ These observations are attributed to the dissociation of the electrostatically bound ion clusters due to competitive interaction of the perchlorate with [Ru(bpy)₃]²⁺ and lithium with [S₂W₁₈O₆₂]⁴⁻.

Scheme 1 provides a model for the formation of 1:1 and 2:1 ion clusters under the conditions employed in the steady state luminescence:

SCHEME 1



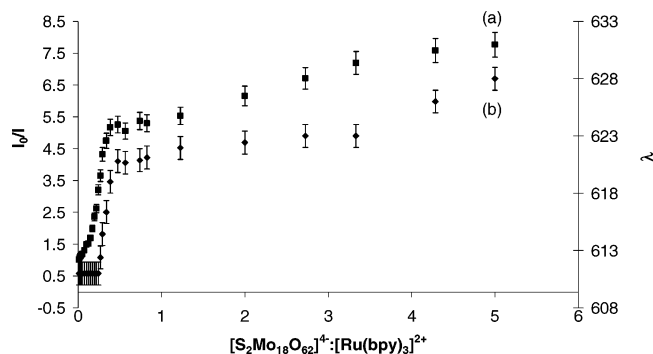


Figure 3. (a) Stern–Volmer plot of luminescence intensity versus ratio of $[\text{S}_2\text{W}_{18}\text{O}_{62}]^{4-}:[\text{Ru}(\text{bpy})_3]^{2+}$. (b) Plot of wavelength versus ratio of $[\text{S}_2\text{W}_{18}\text{O}_{62}]^{4-}:[\text{Ru}(\text{bpy})_3]^{2+}$. Data taken from Figure 1.

The emission data are complicated by the fact that it is the counterion, $[\text{Ru}(\text{bpy})_3]^{2+}$, that is emissive and present in large excess initially. Consequently, the 2:1 ion cluster $[\text{Ru}(\text{bpy})_3]_2\text{S}_2\text{W}_{18}\text{O}_{62}$ is predicted to form first, followed by its dissociation at higher tungstate concentrations to form the 1:1 ion pair $\{[\text{Ru}(\text{bpy})_3][\text{S}_2\text{W}_{18}\text{O}_{62}]\}^{2-}$. Both the 2:1 polymolybdate and polytungstate salts have been isolated in substance, using the method described for the analogue described in ref 8. The higher concentrations of perchlorate required for recovery of luminescent intensity in the polytungstate case are consistent with a higher association constant for the polytungstate ion clusters (vide infra).

The luminescence data were fitted to the Stern–Volmer model (eq 1, Figure 3):

$$\frac{I_0}{I} \quad \text{or} \quad \frac{\tau_0}{\tau} \quad \text{or} \quad \frac{\phi_0}{\phi} = 1 + k_q\tau_0[\text{Q}] \quad (1)$$

where I_0 and I are the luminescence intensities of $[\text{Ru}(\text{bpy})_3]^{2+}$ in the absence and presence of quencher, respectively, τ , τ_0 and ϕ , ϕ_0 are the respective equivalent excited state lifetimes and luminescence quantum yields in the presence and absence of quencher, $[\text{Q}]$ is the concentration of the quenching species, and k_q is the quenching rate constant.

The Stern–Volmer relationship in this form describes dynamic quenching processes. However, for a static process (where a ground state complex is formed between the luminophore and the quencher, which is not luminescent or is only weakly so), the equation is replaced by the relationship given by eq 2:

$$\frac{I_0}{I} = 1 + K[\text{Q}] \quad (2)$$

where K is the association constant.

It is apparent from Figure 3a that at least two distinct regions exist in Stern–Volmer plots. The model indicated in Scheme 1 suggests that the first portion of the plot, where strong emission intensity changes are observed, corresponds to the formation of $[\text{Ru}(\text{bpy})_3]_2[\text{S}_2\text{W}_{18}\text{O}_{62}]$ at mole ratios up to tungstate:Ru ~ 0.5 ([tungstate], $(0-1.9) \times 10^{-6} \text{ mol dm}^{-3}$; [Ru], $5 \times 10^{-6} \text{ mol dm}^{-3}$). Free $[\text{Ru}(\text{bpy})_3]^{2+}$ will also be present in solution in this regime. This first region of the plot was linear up to $6 \times 10^{-7} \text{ mol dm}^{-3} [\text{S}_2\text{W}_{18}\text{O}_{62}]^{4-}$ with an upward deviation from linearity to the second portion of the plot, which commences at $1.9 \times 10^{-6} \text{ mol dm}^{-3} [\text{S}_2\text{W}_{18}\text{O}_{62}]^{4-}$. The positive deviation from linearity is attributed to the fact that the associated complex is itself luminescent. The second data region is linear with a considerably reduced slope compared with the first region. This eventually plateaus at concentrations in excess of $1 \times 10^{-5} \text{ mol}$

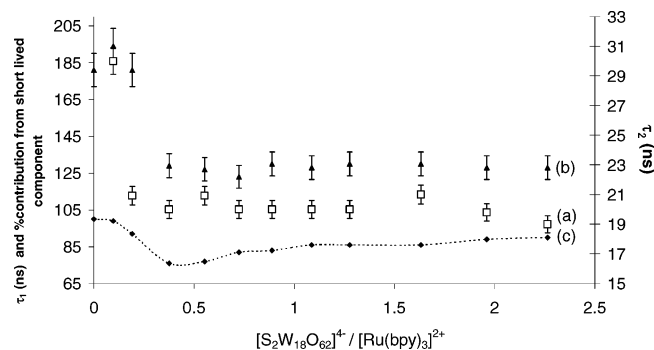


Figure 4. Stern–Volmer plots of time-dependent luminescence data on addition of $[\text{S}_2\text{W}_{18}\text{O}_{62}]^{4-}$ to $[\text{Ru}(\text{bpy})_3]^{2+}$ ($5 \times 10^{-6} \text{ M}$) in acetonitrile: (a) lifetime of short-lived component of decay, \square ; (b) lifetime of long-lived component, \blacktriangle ; (c) percentage contribution of long-lived decay to overall decay, \blacklozenge . Concentrations are expressed as mole ratios of $[\text{S}_2\text{W}_{18}\text{O}_{62}]^{4-}$ to $[\text{Ru}(\text{bpy})_3]^{2+}$.

$\text{dm}^{-3} [\text{S}_2\text{W}_{18}\text{O}_{62}]^{4-}$, consistent with eventual dominance of the 1:1 ion pair. Interestingly, the profile of the Stern–Volmer plot is matched very well by the plot of the λ_{max} of emission (Figure 3b). The initial steep rise of the data, which concludes at a ratio of approximately 0.5:1 of the $[\text{S}_2\text{W}_{18}\text{O}_{62}]^{4-}:[\text{Ru}(\text{bpy})_3]^{2+}$, is therefore attributed to the formation of the 2:1 complex whose λ_{max} value appears to be centered at approximately 630 nm.

Time-Resolved Luminescence. To assess the nature of the quenching interaction between $[\text{S}_2\text{W}_{18}\text{O}_{62}]^{4-}$ and $[\text{Ru}(\text{bpy})_3]^{2+}$, time-resolved luminescence quenching studies were conducted. According to the Stern–Volmer model (eq 1), identical slopes are anticipated for plots of I_0/I and τ_0/τ if the quenching behavior is dynamic.

Plots of the dependence of the luminescent lifetime of $[\text{Ru}(\text{bpy})_3]^{2+}$ on the relative concentration of $[\text{S}_2\text{W}_{18}\text{O}_{62}]^{4-}$ are shown in Figure 4a,b. Two plots are shown for the data because, in contrast to the polymolybdate system,⁴ the addition of $[\text{S}_2\text{W}_{18}\text{O}_{62}]^{4-}$ causes the luminescence lifetime decays to become biexponential.¹¹ Plots a and b of Figure 4 show the lifetime of the short- and long-lived components of decay, respectively. The short-lived component appears after the first addition of tungstate and does not, within experimental error, change with further addition of tungstate; the long-lived component exhibits an initial step at $1.88 \times 10^{-6} \text{ M}$ tungstate, corresponding to $[\text{S}_2\text{W}_{18}\text{O}_{62}]^{4-}:[\text{Ru}(\text{bpy})_3]^{2+} \sim 1:3$, after which no further concentration dependence is observed.

The first step can be attributed to the presence of free $[\text{Ru}(\text{bpy})_3]^{2+}$ which will be present in excess at this initial stage of the titration. Figure 4c shows the percentage contribution of the long-lifetime component to the overall decay. As the relative concentration of tungstate increased, the intensity of the long-lived component gradually decreased as more of the $[\text{Ru}(\text{bpy})_3]^{2+}$ participated in quenching interactions. This contribution is minimized at $[\text{S}_2\text{W}_{18}\text{O}_{62}]^{4-}:[\text{Ru}(\text{bpy})_3]^{2+} \sim 0.5$ (1:2) and then proceeds to increase. The increase coincides with a stepped decrease in the lifetime of this long-lived component from approximately 190 to 130 ns, a value which remains constant at higher relative concentrations of tungstate.

As the short-lived component appears only after the initial addition of tungstate, it is attributed to luminescence from the $[\text{Ru}(\text{bpy})_3]_2[\text{S}_2\text{W}_{18}\text{O}_{62}]$ ion cluster. In the equivalent polymolybdate system, quenching was found to be entirely static, as τ was observed to be independent of polymolybdate concentration.⁴ The behavior reported here is more complex as the ion cluster appears to have a luminescence whose lifetime is approximately 20 ns (± 2 ns), although this is independent of

TABLE 1: Association Constants K_n for $[\text{Ru}(\text{bpy})_3]_n[\text{S}_2\text{M}_{18}\text{O}_{62}]$ Estimated from Fluorescence and Absorption Data

method	$[\text{S}_2\text{W}_{18}\text{O}_{62}]^{4-}$		$[\text{S}_2\text{Mo}_{18}\text{O}_{62}]^{4-}$	
	$K_1 (\times 10^{-4}), \text{mol}^{-2} \text{dm}^{-6}$	$K_2 (\times 10^{-4})$	$K_1 (\times 10^{-4}), \text{mol}^{-2} \text{dm}^{-6}$	$K_2 (\times 10^{-4})$
Stern–Volmer	180	14	40	3
Bourson–Valeur eq (fluorescence)	290	44	58	1.3
Bourson–Valeur eq (absorption)	100	77	35–70	2.5

tungstate concentration. In the analogous polymolybdate adduct, no such decay was observed as the luminescent lifetime of the cluster was <5 ns and outside the range of our instrumentation.¹² The long-lived component of the decay is also independent of tungstate concentration up to $[\text{S}_2\text{Mo}_{18}\text{O}_{62}]^{4-}:[\text{Ru}(\text{bpy})_3]^{2+} \sim 0.5$ (1:2). The origin of the abrupt decrease in luminescence lifetime at this concentration is unclear. However, it also corresponds to a minimum in the contribution of the long-lived component to the overall decay (Figure 4b). At this mole ratio, according to estimates of the association constant for $[\text{Ru}(\text{bpy})_3]_2\text{-}[\text{S}_2\text{W}_{18}\text{O}_{62}]$ (vide infra), only 1 equiv of free $[\text{Ru}(\text{bpy})_3]^{2+}$ ion exists in solution per 10^6 equiv of the adduct. At higher relative concentrations of tungstate, the 1:1 ion pair $\{[\text{Ru}(\text{bpy})_3]\text{-}[\text{S}_2\text{W}_{18}\text{O}_{62}]\}^-$ will start to form (Scheme 1). One possibility is that the reduction in the lifetime of the long-lived component is due to the presence of this ion pair.

Whatever the origin of this complexity in the lifetime behavior, both the short- and long-lived components are independent of tungstate concentration, indicative of purely static quenching. The static nature of the interaction between $[\text{S}_2\text{W}_{18}\text{O}_{62}]^{4-}$ and $[\text{Ru}(\text{bpy})_3]^{2+}$ can also be inferred from the effect of ionic strength on the quenching behavior (Figure 2).

Electronic Spectroscopy and Association Constants. An unexpected feature of the polymolybdate system was the presence of a new charge-transfer transition centered at 485 nm, attributed to the $[\text{Ru}(\text{bpy})_3]_2[\text{S}_2\text{Mo}_{18}\text{O}_{62}]$ ion cluster.⁴ The polytungstate system was also examined using difference electronic spectroscopy to follow the addition of $[\text{S}_2\text{W}_{18}\text{O}_{62}]^{4-}$ to $[\text{Ru}(\text{bpy})_3]^{2+}$ in dry acetonitrile (Figure 5). A new absorption band, not observed in the polytungstate or $[\text{Ru}(\text{bpy})_3]^{2+}$ ions alone, developed at 474 nm, indicative of strong electronic communication between the $[\text{S}_2\text{W}_{18}\text{O}_{62}]^{4-}$ and $[\text{Ru}(\text{bpy})_3]^{2+}$ ions. In addition to identifying the new optical transition, these experiments allowed estimation of association constants (Scheme 1). From the model of ground state association described in eq 2, a plot of (I_0/I) vs polytungstate concentration provides a slope K which can be used to estimate the association constant. The slopes of the two linear regions in the plots of I_0/I vs $[Q]$ give

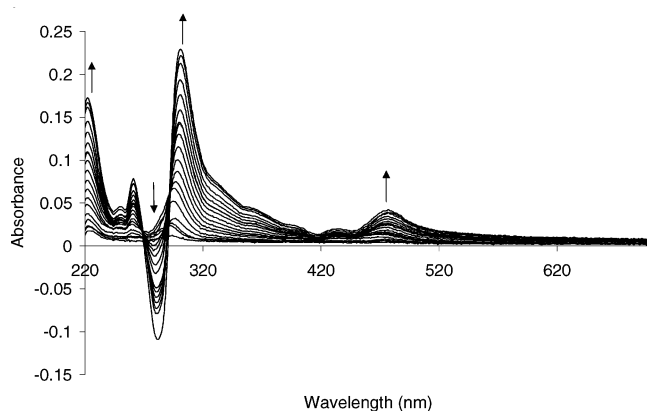


Figure 5. Difference electronic spectra for titration of $[\text{S}_2\text{W}_{18}\text{O}_{62}]^{4-}$ into $[\text{Ru}(\text{bpy})_3]^{2+}$ in acetonitrile. The spectra were generated by subtracting the spectra of the separate solutions from the experimental spectrum of the mixture. The process was carried out as a function of increasing concentration of $[\text{S}_2\text{W}_{18}\text{O}_{62}]^{4-}$.

the association constants for the 2:1 and 1:1 complexes and are shown in Table 1. The values found for the polymolybdate system are listed for comparison.

A more accurate method for estimation of association constants is described by the Bourson and Valeur expression, eq 3:

$$\frac{I_F^0}{I_F^0 - I_F} = \frac{\epsilon_{\text{Ru}}\Phi_{\text{Ru}}}{\epsilon_{\text{Ru}}\Phi_{\text{L}} - \epsilon_{\text{RuW}}\Phi_{\text{RuW}}\left(\frac{1}{K_s[W]} + 1\right)} \quad (3)$$

where subscripts Ru, W, and RuW refer to $[\text{Ru}(\text{bpy})_3]^{2+}$, $[\text{S}_2\text{W}_{18}\text{O}_{62}]^{4-}$, and $[\text{Ru}(\text{bpy})_3]_2[\text{S}_2\text{W}_{18}\text{O}_{62}]$, respectively. From a plot of $I_F^0/(I_F^0 - I_F)$ vs $[W]$ the stability constant can be calculated from the ratio of the intercept:slope. This plot shows a graph that is initially linear and whose slope increases after the cation:anion ratio is less than 4.1:1. The intercept:slope ratio is $4.4 \times 10^5 \text{ dm}^3 \text{ mol}^{-1}$ rising to $2.9 \times 10^6 \text{ dm}^3 \text{ mol}^{-1}$. The values of K_1 and K_2 derived in this manner are also listed in Table 1.

Equation 3 also can be applied to the absorbance data, in the rearranged form given below.

$$\frac{A_0}{A_0 - A} = \frac{\epsilon_{\text{L}}}{\epsilon_{\text{L}} - \epsilon_{\text{ML}}\left(\frac{1}{K_s[M]} + 1\right)} \quad (4)$$

From a plot of $A_0/(A_0 - A)$ vs $1/[M]$, the association constants can be calculated from the ratio of the intercept:slope. In the case of absorption data, $[\text{Ru}(\text{bpy})_3]^{2+}$ was titrated into $[\text{S}_2\text{W}_{18}\text{O}_{62}]^{4-}$ solution, initially forming the 1:1 complex. The derived value for K_2 was 7.7×10^5 . In the reverse titration, the 2:1 complex forms initially and the derived value of K_1 was $1.0 \times 10^6 \text{ mol}^{-2} \text{ dm}^{-6}$. Table 1 shows these data and those estimated for the polymolybdate system.

Excellent agreement is observed between the different estimates of the association constants (Table 1). Those for the polytungstate system are approximately an order of magnitude higher than those for the polymolybdate system, consistent with the conclusions of the ionic strength studies. As the materials are structurally analogous, the origin of this difference is unclear, particularly since W(VI) is more electropositive than Mo(VI),¹³ and consequently, polyoxotungstate anions are expected to be less basic than their polymolybdate analogues.⁷

Excitation Spectroscopy. The new optical transition observed in the difference absorbance spectrum may result in a luminescent state. Excitation spectra (emissive intensity versus excitation wavelength) were examined under the same conditions as those employed for the luminescence titration. Initially and at low relative concentrations of polytungstate, the excitation spectrum is typical of $[\text{Ru}(\text{bpy})_3]^{2+}$ luminescence, with λ_{max} centered around 450 nm (Figure 6). However, for increasing concentrations of polytungstate, the 450 nm feature decreases in intensity and a new absorbance band, centered around 480 nm, grows in. This wavelength corresponds to the new absorbance feature observed at 474 nm in the difference spectra described above. The data indicate that this transition leads to a luminescent state. The excitation band reaches maximum intensity at $[\text{S}_2\text{W}_{18}\text{O}_{62}]^{4-}:[\text{Ru}(\text{bpy})_3]^{2+} \sim 1:2$ and decreases for ratios above 1:1. This

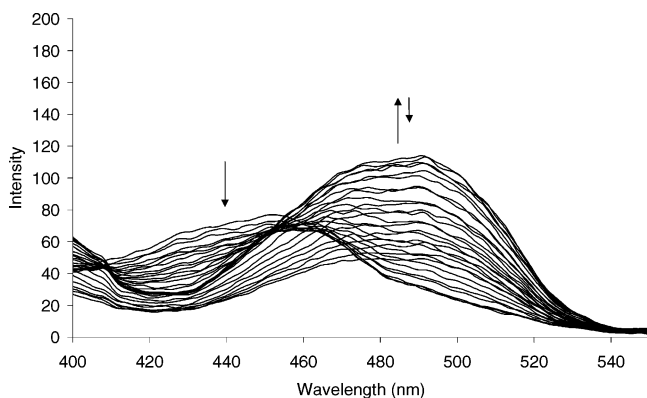


Figure 6. Uncorrected excitation spectra in dry acetonitrile for $[\text{Ru}(\text{bpy})_3]^{2+}$ and $(1 \times 10^{-5} \text{ M}) [\text{S}_2\text{W}_{18}\text{O}_{62}]^{4-}$. Detecting at (a) 590 and (b) 650 nm.

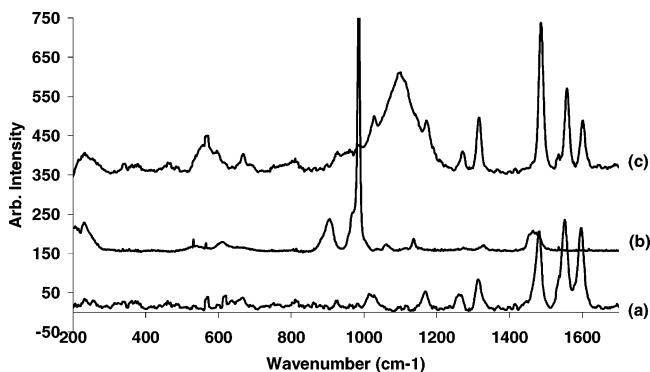


Figure 7. Resonance Raman spectroscopy of $[\text{Ru}(\text{bpy})_3]_2[\text{S}_2\text{W}_{18}\text{O}_{62}]^{4-}$, 5% dispersed in KBr, excited at 457.9 nm. (a) $[\text{Ru}(\text{bpy})_3](\text{PF}_6)_2$; (b) $[\text{Hex}_4\text{N}]_4[\text{S}_2\text{W}_{18}\text{O}_{62}]^{4-}$; (c) $[\text{Ru}(\text{bpy})_3]_2[\text{S}_2\text{W}_{18}\text{O}_{62}]^{4-}$.

decrease in excitation intensity is attributed to the decreasing luminescence of the solution at higher polytungstate concentrations rather than loss of the 475 nm band, since the latter persisted over all polytungstate concentrations examined in the difference absorbance spectra. The observations suggest that this transition is associated with the $[\text{Ru}(\text{bpy})_3]_2[\text{S}_2\text{W}_{18}\text{O}_{62}]$ ion cluster, which is itself luminescent.

Resonance Raman Spectroscopy. This technique was employed to assign the origin of the new optical transition apparent in both the electronic absorption and excitation spectra. Excitation wavelengths coincident or resonant with the absorbance under interrogation leads to resonance enhancement by up to 7 orders of magnitude of the Franck–Condon modes of the chromophore.¹⁴ Figure 7 shows the solid state Raman spectra of $[\text{Ru}(\text{bpy})_3]\text{Cl}_2$, $[\text{Hex}_4\text{N}]_4[\text{S}_2\text{W}_{18}\text{O}_{62}]^{4-}$, and the 2:1 ion cluster, $[\text{Ru}(\text{bpy})_3]_2[\text{S}_2\text{W}_{18}\text{O}_{62}]$, which may be isolated as a solid. The excitation wavelength was 457.9 nm, which is preresonant with the new optical transition observed at 474 nm and assigned to the ion cluster. The intensities of the three spectra are normalized as $[\text{S}_2\text{W}_{18}\text{O}_{62}]^{4-}$ is not resonant at 457.9 nm and its spectrum is considerably weaker. $[\text{Ru}(\text{bpy})_3]^{2+}$ exhibits the typical signature of seven vibrations associated with the bipyridyl ligands as well as a Ru–N mode at 370 cm^{-1} , typical of resonance with the metal to ligand charge transfer (MLCT) transition.¹⁵ $[\text{S}_2\text{W}_{18}\text{O}_{62}]^{4-}$ exhibits a number of WO and SO stretching modes at, respectively, 987 and 897 cm^{-1} and 1058 and 1131 cm^{-1} . In addition, OWO bending modes occur at 597 and 520 cm^{-1} . Bands associated with the quaternary ammonium cation occur at 1322 and 1461 cm^{-1} .¹⁶ Figure 7c shows that the 2:1 salt possesses the signature bipyridyl modes but, in addition, new features are enhanced that are not present in the

$[\text{Ru}(\text{bpy})_3]^{2+}$ spectrum. A broad new feature is apparent at 1093 cm^{-1} , and other features appear at 980 , 922 , 586 , and 561 cm^{-1} . These new features are assigned to the polytungstate anion, but are shifted somewhat in comparison to $[\text{Hex}_4\text{N}]_4[\text{S}_2\text{W}_{18}\text{O}_{62}]$ (Figure 7b). Their enhancement indicates that, in parallel with $[\text{Ru}(\text{bpy})_3]_2[\text{S}_2\text{Mo}_{18}\text{O}_{62}]^{4-}$, the transition at 470 nm may be assigned to a $[\text{Ru}(\text{bpy})_3]^{2+}$ to $[\text{S}_2\text{W}_{18}\text{O}_{62}]^{4-}$ charge-transfer transition.

Photochemical Stability and Temperature Dependence of Photophysics. We have reported the remarkable photochemical stability of the $[\text{Ru}(\text{bpy})_3]_2[\text{S}_2\text{Mo}_{18}\text{O}_{62}]$ ion cluster.⁴ Photolysis studies on $[\text{Ru}(\text{bpy})_3]_2[\text{S}_2\text{W}_{18}\text{O}_{62}]$ were undertaken in light of its complementary optical behavior. Continuous photolysis using a 300 W Xe arc lamp over a 4 h period showed no significant change in the spectrum in acetonitrile. For comparison, $[\text{Ru}(\text{bpy})_3]^{2+}$ was photolyzed under the same conditions and underwent greater than 40% conversion to the acetonitrile-substituted decomposition product over the same period of time.¹⁷ The photostability of these ion clusters may be attributed to a number of factors. First, as the new optical transitions occur at a wavelength which is approximately 0.12 eV lower in energy than the lowest optical transition in free $[\text{Ru}(\text{bpy})_3]^{2+}$, it is possible that the lower energy excited state in the adduct causes the destructive triplet metal-centered state to be thermally inaccessible. Alternatively, fast photoinduced electron transfer from $[\text{Ru}(\text{bpy})_3]^{2+}$ to the polyoxometalate anion may outrun the photodecomposition reaction. Studies of the temperature dependence of the photophysics of the $[\text{Ru}(\text{bpy})_3]_2[\text{S}_2\text{W}_{18}\text{O}_{62}]$ ion cluster were initiated to obtain further insight into the origin of the photostability.

Temperature-dependent photophysical data on polypyridylruthenium complexes has been used to provide insight into appropriate models for deactivation behavior. Over a relatively modest temperature range, the observed radiative rate constant may be fitted to eq 5:

$$k_{\text{obs}} = k_0 + A' \exp\left(\frac{-\Delta E}{RT}\right) \quad (5)$$

where k_{obs} is the observed rate constant for radiative decay, $k_0 = k_{\text{nr}}$ (nonradiative decay constant) + k_{r} (radiative decay constant), A' is a preexponential factor associated with the frequency of activated surface crossing, and ΔE is the activation energy for surface crossing.

In general, polypyridylruthenium complexes fall into one of two categories according to their temperature-dependent behavior: (i) small activation energy ($< 800 \text{ cm}^{-1}$) and low preexponential factor ($< 10^9 \text{ s}^{-1}$) or (ii) large activation energy ($> 2000 \text{ cm}^{-1}$) and large preexponential factor ($< 10^{12} \text{ s}^{-1}$). Complexes exhibiting behavior (i) are typically photochemically inert as the low prefactor has been associated with thermal population of a weakly coupled fourth MLCT state which has significant singlet character.¹⁸ For behavior (ii), the complex is typically photoactive, as in the case of $[\text{Ru}(\text{bpy})_3]^{2+}$, which undergoes activated surface crossing to a triplet metal-centered state which leads to ligand loss.¹⁹

A complication of the temperature dependent lifetime studies is that the association constants estimated for the ion clusters would be expected to be temperature dependent. This would be expected to affect only the preexponential terms in the decay fit (i.e., a or b ¹¹) as alterations to the association constant are not anticipated to alter the observed lifetimes. The individual lifetimes of the complexes were calculated according to a biexponential model as described above (see Figure 4). Figure 8 shows the temperature dependence of the luminescent lifetime

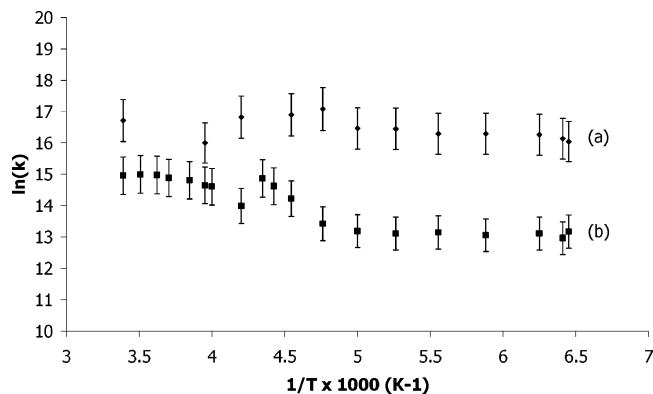


Figure 8. Temperature-dependent luminescent data for mole ratio 2.5:1 $[\text{Ru}(\text{bpy})_3]_2[\text{S}_2\text{W}_{18}\text{O}_{62}]$, in 4:5 butyronitrile:propionitrile: (a) short component; (b) long component. Concentration of $[\text{Ru}(\text{bpy})_3]^{2+} = 5 \times 10^{-6}$ M.

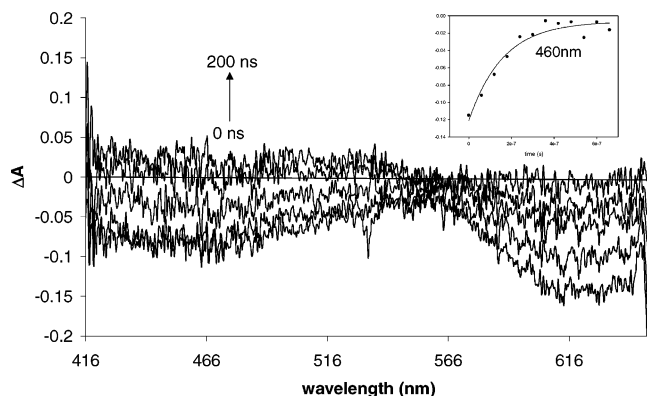


Figure 9. Transient absorption of $[\text{Ru}(\text{bpy})_3]_2[\text{S}_2\text{W}_{18}\text{O}_{62}]$ in acetonitrile 0, 60, 120, 180, and 420 ns after excitation at 355 nm.

for a solution containing a 2:1 molar ratio of $[\text{Ru}(\text{bpy})_3]^{2+}$ (2×10^{-5} M) and $[\text{S}_2\text{W}_{18}\text{O}_{62}]^{4-}$ (1×10^{-5} M) Figure 8a shows the results for the fast-decaying component of the decay and Figure 8b the temperature dependence of the long-lived component of the decay. Fitting the temperature-dependent portion of Figure 8a to the Arrhenius expression gives $A = 3.02 \times 10^6 \text{ s}^{-1}$ and $E_a = 207 \text{ cm}^{-1}$, compared with $E_a = 3800 \text{ cm}^{-1}$ for free $[\text{Ru}(\text{bpy})_3]^{2+}$ in acetonitrile.²⁰ These values reflect the excellent photostability of this complex and are reminiscent of photostable polypyridylruthenium complexes (case (i) above).²¹ Figure 8b shows similar behavior for $[\text{Ru}(\text{bpy})_3]^{2+}$ with A approximately 10^{10} s^{-1} and $E_a = 3670 \text{ cm}^{-1}$. This appears to confirm that the long-lived component in the concentration range corresponding to the presence of $[\text{Ru}(\text{bpy})_3]_2[\text{S}_2\text{W}_{18}\text{O}_{62}]$ (Figure 4) is due to free $[\text{Ru}(\text{bpy})_3]^{2+}$. That this complex remains evident in luminescent experiments given the large association constant with the polytungstate may seem surprising. However, the luminescence quantum yield of $[\text{Ru}(\text{bpy})_3]^{2+}$ is high and is likely to be considerably larger than that of the bound adduct. Therefore, even if present at very low concentrations, it can dominate the luminescence intensity.

Transient Absorption Spectroscopy. Preliminary transient spectroscopy was undertaken on the polytungstate–ruthenium ion cluster. Figure 9 shows the transient absorption spectra of a 2:1 molar ratio solution of $[\text{Ru}(\text{bpy})_3]^{2+}$ and $[\text{S}_2\text{W}_{18}\text{O}_{62}]^{4-}$. Depletions are observed at 620 and 460 nm, corresponding to the luminescence from the $[\text{Ru}(\text{bpy})_3]_2[\text{S}_2\text{W}_{18}\text{O}_{62}]$ ion cluster and depletion of the charge-transfer transition. A first-order kinetic fit of data taken from the time dependence of the 460 nm depletion yields $k = 6.27 \times 10^6 \text{ s}^{-1}$, i.e., a lifetime of 160

ns. This corresponds reasonably well to the lifetime of the long-lived component of the luminescence lifetime. However, comparison of the transient spectrum with that of $[\text{Ru}(\text{bpy})_3]^{2+}$ leads to the conclusion that the width of the visible depletion is considerably broader than expected and is shifted approximately 25 nm to the red (see Supporting Information). This is consistent with the excitation and difference spectra, which suggests that a new optical transition is involved, although the lifetime is longer than expected based on the short-lived component of the luminescence. In the analogous polymolybdate cluster, a new optical transition grew in centered around 600 nm, which was attributed to the reduced polymolybdate. Such a feature was not observed here, which may be due to the fact that the polytungstates are considerably more difficult to reduce or because the feature was masked by the luminescence from this material, which was not observed in the polymolybdate transient absorption data.²² We are currently investigating the time-resolved spectroscopy of the polytungstate and polymolybdate clusters in further detail.

Conclusions

The photophysical and spectroscopic properties of $[\text{Ru}(\text{bpy})_3]_2[\text{S}_2\text{W}_{18}\text{O}_{62}]$ are described and compared with those of the polymolybdate analogue. There are strong similarities in the behavior of the two adducts: both clusters appear to be primarily electrostatic bound, but exhibit new optical transitions leading to luminescent states which are considerably shorter lived than the $[\text{Ru}(\text{bpy})_3]^{2+}$ alone. This extent of electronic communication, and in particular the presence of a new luminescent state arising out of the adduct species, appears to be limited to the Dawson sulfo-polyoxometalates, as it has not been observed other polyoxometalate species.^{10,23}

The adducts exhibit photostability under the conditions explored where $[\text{Ru}(\text{bpy})_3]^{2+}$ exhibited considerable photolability. Temperature-dependent luminescence studies in combination with UV–vis spectroscopy suggest that alteration to the $[\text{Ru}(\text{bpy})_3]^{2+}$ energy levels may be responsible, rather than fast electron transfer, which outruns the photodecomposition reaction. The main difference between the polytungstate and polymolybdate complexes lies in the association constant with $[\text{Ru}(\text{bpy})_3]^{2+}$ which is an order of magnitude higher for the polytungstate. The λ_{max} of the new charge-transfer transition lies approximately 10 nm to the blue of the polymolybdate complex, and the luminescent lifetime of $[\text{Ru}(\text{bpy})_3]_2[\text{S}_2\text{W}_{18}\text{O}_{62}]$ appears to be significantly longer than that of the polytungstate analogue.

Acknowledgment. We gratefully acknowledge the Australian Research Council for funding. T.E.K., M.K.S., L.G., and R.J.F. gratefully acknowledge Enterprise Ireland under grant SC/2002/149. Part of this work was conducted at FOCAS, DIT funded under the National Development Plan 2000 to 2006. T.E.K. gratefully acknowledges Johnson Matthey for the generous loan of RuCl_3 .

Supporting Information Available: Transient spectra of $[\text{Ru}(\text{bpy})_3]^{2+}$ alone and $[\text{Ru}(\text{bpy})_3]_2[\text{S}_2\text{W}_{18}\text{O}_{62}]$ in acetonitrile taken 50 ns after 355 excitation pulse. This material is available free of charge via the Internet at <http://pubs.acs.org>.

References and Notes

- (1) (a) Müller, M. T. In *Polyoxometalates: From Platonic Solids to Anti-Retroviral Activity*; Pope, A., Ed.; Kluwer Academic Publishers: Dordrecht, 1994. (b) Hill, C. L. In *Comprehensive Coordination Chemistry II*; Wedd, A. G.; Ed.; Elsevier: Oxford, 2004; Vol. 4, pp 679–759.

- (2) Ruther, T.; Hultgren, V. M.; Timko, B. P.; Bond, A. M.; Jackson, W. R.; Wedd, A. G. *J. Am. Chem. Soc.* **2003**, *125*, 10133.
- (3) Bond, A. M.; Way, D. M.; Compton, R. G.; Booth, J.; Eklund J. C.; Wedd, A. G. *Inorg. Chem.* **1995**, *34*, 3378–3384. Reduced forms of these anions appear to be photoactive in the visible region via intervalence transitions.
- (4) Keyes, T. E.; Gicquel, E.; Guerin, L.; Hultgren, V.; Wedd, A. G.; Bond, A. M. *Inorg. Chem.* **2003**, *24*, 7897.
- (5) Palmer, R. A.; Piper, T. S. *Inorg. Chem.* **1966**, *5*, 864.
- (6) Cooper, J. B.; Way, D. M.; Bond, A. M.; Wedd, A. G. *Inorg. Chem.* **1993**, *32*, 2416.
- (7) Richardt, P. J. S.; Gable, R. W.; Bond, A. M.; Wedd, A. G. *Inorg. Chem.* **2001**, *40*, 703.
- (8) Hultgren, V. M.; Bond, A. M.; Wedd, A. G. *J. Chem. Soc., Dalton Trans.* **2001**, 1076.
- (9) Diamond, D.; Hanratty, V. *Excel for Chemists*; John Wiley & Sons–VCH: New York, 1997.
- (10) Ballardini, R.; Gandolfi, M. T.; Balzani, V. *Inorg. Chem.* **1987**, *26*, 862.
- (11) Data were modeled according to the equation $I(t) = a \exp(-k_1 t) + b \exp(-k_2 t) + c$, where $I(t)$ is luminescence intensity as a function of time, a and b are preexponential factors, k_1 and k_2 are the observed radiative decay rate constants, and c is background.
- (12) If a dynamic collisional component coexisted with a static process, the component of the lifetime due to the unbound $[\text{Ru}(\text{bpy})_3]^{2+}$ would be expected to vary with tungstate concentration. That a concentration-independent component remains suggests that all available tungstate is bound and unavailable for collisional interactions with the remaining $[\text{Ru}(\text{bpy})_3]^{2+}$.
- (13) Huhey, J. E.; Keiter, E. A.; Keiter, R. *Inorganic Chemistry*, 4th ed.; Harper-Collins: New York, 1993; pp 189–190.
- (14) Ferraro J.; John, R. *Introduction to Raman Spectroscopy*; Academic Press: New York, 1994.
- (15) Coates, C. G.; Keyes, T. E.; Hughes, H. P.; Jayaweera, P. M.; McGarvey, J. J.; Vos, J. G. *J. Phys. Chem. A* **1998**, *102*, 5013.
- (16) Botto, I. L.; Garcia, A. C.; Thomas, H. J. *J. Phys. Chem. Solids* **1992**, *53*, 1075.
- (17) Durham, B.; Casper, J. V.; Nagel, J. K.; Meyer, T. J. *J. Am. Chem. Soc.* **1982**, *104*, 4803.
- (18) Juris, A.; Balzani, V.; Barigelletti, F.; Campagna, S.; Belser, P.; Von Zelewsky, A. *Coord. Chem. Rev.* **1988**, *84*, 85.
- (19) Allsopp, S. R.; Cox, A.; Kemp, T. J.; Reed, W. J. *J. Chem. Soc., Faraday Trans.* **1978**, *74*, 1275.
- (20) Casper, J. V.; Meyer, T. J. *J. Am. Chem. Soc.* **1983**, *105*, 5583.
- (21) Keyes, T. E.; Vos, J. G.; Kolnaar, J. A.; Haasnoot, J.; Reedijk, J.; Hage, R. *Inorg. Chim. Acta* **1996**, *245*, 237.
- (22) Steady state photolysis studies of the ion clusters showed no evidence for the formation of a stable one-electron-reduced tungstate. This is not surprising, however, as it is likely that fast charge recombination will occur between any electron-transfer product of the ruthenium polypyridyl complex and the tungstate, due to their increased electrostatic association.
- (23) Seery, M. K.; Fay, N.; McCormac, T.; Dempsey, E.; Keyes, T. E. Photophysics of Ruthenium Polypyridyl Complexes with Phosphopolyoxotungstates. Manuscript in preparation.